Conformation of Surface-Bound Polyelectrolytes. 2. A Monte Carlo Study of Medium-Length Lattice Chains

M. K. Granfeldt,† S. J. Miklavic,*,†,‡ S. Marčelja,‡ and C. E. Woodward†

Physical Chemistry 2, Chemical Center, P.O. Box 124, S-221 00, Lund, Sweden, and Department of Applied Mathematics, Research School of Physical Sciences, Australian National University, Canberra, 2061, ACT, Australia

Received March 7, 1989; Revised Manuscript Received April 11, 1990

ABSTRACT: A combination of a Monte Carlo technique and mean-field theory is used to study the interaction of two planar surfaces bearing *end*-attached polyelectrolytes. The latter are modeled as flexible, linear chains whose self-avoiding configurations are superimposed on a tetrahedral lattice. Electrostatic interactions are taken into account via a mean-field potential that satisfies an extended Poisson–Boltzmann equation, while chain excluded volume effects are included via avoidance sampling of configurations. A mean-field potential energy expression is used to study the interaction of the two surfaces. Examples of the dependence of the monomer distribution, electrostatic potential, and the interaction potential on the effective polyelectrolyte charge, surface charge, and salt concentration are presented. The interaction potential acting between these two surfaces exhibits the influence of many competing effects arising from the presence of charged chains and is significantly different from either the interaction of surfaces with grafted neutral chains or the usual double-layer interaction between two charged planes.

Introduction

We consider the manner by which forces acting on and between large colloidal particles are modified by the presence of flexible polymers and polyelectrolytes.[1] The behavior and influence of polysaccharide or protein cell coats on the interaction of cell bodies and the latter's response to external potentials are of enormous importance. For example, it is now recognized that surface-attached polyelectrolytes play an important role in the electrophoretic response of biological cells.[2] While such events involve highly complex functions, both specific and nonspecific, we demonstrate here the possibility of quantifying the nonspecific role polyelectrolytes play in interaction phenomena, at a reasonably simple level.

A large number of experimental and theoretical studies of systems involving polymers near interfaces have appeared in the literature. Those systems involving polymers attached, i.e., grafted, to surfaces are of particular interest. Theoretical calculations employ a variety of techniques to solve this many-body problem ranging from lattice and off-lattice simulations of polymer chains[3-9] to scaling principles[10-12] to continuum, self-consistent field theories.[13-17] While the simulations are often limited to chains of low to medium molecular weight, the excluded volume problem of polymers is generally treated explicitly. When seen in comparison, the self-consistent theories are shown to be limited to regimes of weak excluded volume interaction. They have, however, the advantage of being relatively easy and quick to implement. In many cases, the results of force calculations based on these theoretical models are found to be comparable with measured forces between mica surfaces bearing nonionic polymers (adsorbed or attached) immersed in different solvents.[18-24]

In contrast to neutral polymers one finds that by placing a large number of ionizable groups sequentially along the backbone of a polymer chain, all of its conformational properties are significantly modified. The long-range Coulombic interactions among the bound charges directly affect macromolecular conformations while the presence of the charges creates a nonuniform distribution of the electrolyte ions present in solution which serves to screen the bound charges. The final conformational state of a polyelectrolyte chain lies somewhere between the fully stretched limit and the neutral polymer. The strong coupling between the distributions of monomers and electrolyte species suggests that in order to obtain any equilibrium property, one must consider both distributions simultaneously. While a few studies of forces mediated by a polyelectrolyte have been conducted (both experimental[25,26] and theoretical[27,28]), further clarifying work is needed.

One appealing approach is to model a polyelectrolyte molecule as a series of point charges connected by an appropriate bonding function, the resulting chain then allowed to sample regions of configuration space consistent with the action of this function. Such models have already been implemented in simulations of bulk polyelectrolyte solutions[29-31] and, in one instance, for the inhomogeneous problem of a polyelectrolyte solution between two charged surfaces.[28] As in the latter case, our work aims to investigate an inhomogeneous problem: the interaction of surfaces bearing end-attached polyelectrolytes. Our approach differs from the above in that, rather than take explicit account of direct Coulombic interactions, we implement a mean-field approximation, based on the Poisson–Boltzmann formalism of simple electrolyte theory,[32] to the case of connected ions and combine this with lattice simulation techniques previously used in studies of neutral polymer systems.[33-39] The two calculations are combined into a self-consistent description of distributions.

Once self-consistency is satisfied we employ the equilibrated monomer densities and mean-field electrostatic potential profiles to a calculation of the interaction free energy of a system of two charged, polyelectrolyte "coated" surfaces. Examples of this interaction potential are presented here as a function of surface separation in different cases of chain length, coverage and charge, surface charge, and electrolyte concentration.

The Computational Model

In the present study we consider the two cases of a single, charged planar surface and of two interacting planar

* To whom correspondence should be addressed.
† Physical Chemistry 2, Chemical Center.
‡ Department of Applied Mathematics, Research School of Physical Sciences, Australian National University.

0024-9297/90/2223-4760$02.50/0

surfaces, each with some specified number of end-grafted charged chains (per unit area). The surfaces are in contact with a simple uni-univalent electrolyte solution.

To obtain polymer conformations we use a biased random walk procedure and generate an ensemble of configurations for a surface of attached chains with monomers positioned on vertices of a tetrahedral lattice. As polyelectrolytes possess both charged and neutral groups that are themselves composed of several atoms, we consider, to a first approximation, the finite size of repeat units while the mobile electrolyte species remain point particles. To this end we account for the volume exclusion of monomers explicitly by including only nonoverlapping configurations in our ensemble.

The solution of the electrostatic problem is based on Poisson's equation of electrostatics.[40] The average potential, ψ, is determined by both the charge from the polyelectrolyte molecules and any simple electrolyte. Chain configurations are consequently weighted by a sum of energy terms proportional to the values of ψ at the positions of monomers. These calculations are made self-consistent.

With the electrostatic problem treated at the mean-field level one further, computational approximation to the nonoverlap of chains effectively reduces the original, and formidable, *multi*chain problem to the case of a system of independent, *single* chains. In this approximation one simply mimics the direct steric interaction between chains on the same surface thus: a single chain is placed in a cell with periodic boundaries, with the size of the cell determined by the density of chains on the surface. The final distribution function for the full system is then simply proportional to that for a single chain attached to the surface, with proportionality given by the density of chains on the surface. Details of these calculations are provided below.

A. The Sampling Algorithm and Configuration Probabilities. Our interest in the properties of reasonably long, linear macromolecules necessitates the use of Monte Carlo (MC) methods for the evaluation of chain statistics. We obtain an ensemble of configurations of a *single* chain from a series of self-, neighbor-, and wall-avoiding random walks (i.e., all-avoiding walks (AAW)) on a tetrahedral lattice.[3,37,38] We have selected the diamond lattice for two reasons. First, chain configurations on this lattice have a structure reminiscent of the backbone of real polymers. Second, this lattice provides the lowest coordination number. Only 3 possibilities exist for each step and, for the case of an otherwise unrestricted N-step walk, this results in at most 3^N possible configurations.

The surface-bound monomer (labeled "0") is placed at the origin of a Cartesian coordinate system, while each subsequent monomer ($1 \le i \le N$) is located at coordinates (a_i, b_i, c_i) with respect to this system. The surface normal vector is $\mathbf{n} = (0, 1/\sqrt{2}, 1/\sqrt{2})$. If 4λ is given as the length of the unit cell, then $\sqrt{3}\lambda$ is the length of each bond. Successive steps of the walk are obtained by a random choice among the three *directions* $[-\alpha, \beta, \gamma]$, $[\alpha, -\beta, \gamma]$, or $[\alpha, \beta -\gamma]$ from the preceding site whenever the latter is reached in the direction $[\alpha, \beta, \gamma]$ from *its* predecessor. Here $\alpha, \beta, \gamma = \pm 1$. For such a random step to be acceptable, certain criteria must be satisfied.

First, with the surface being impenetrable, no part of the chain or walk can lie below the plane, $z = (b + c)/2 = 0$. Second, there is the constraint that no site on the lattice can be occupied by more than one monomer. This restriction results in a self-avoiding walk.

A third consideration concerns the possibility of interactions with neighboring chains. If the number of chains per unit area on the surface, i.e., the grafting density, ϑ, is sufficiently low that the distance between grafting points ($\sim \vartheta^{-1/2}$) is much larger than the equilibrium length of the chain, then there are no steric obstructions caused by other chains and a chain must only avoid itself and the surface. If, on the other hand, ϑ is high, many hard-core encounters with neighbors occur. To account for this one may simply enclose the chain in a box with walls that can be treated as either hard or periodic. The actual size of the box is determined by the surface area allocated to each chain, equal to ϑ^{-1}. A box with hard walls is the more restrictive case as it obviates the possibility of any chain entanglement. Periodicity, however, implies that any part of the chain emerging from one side of the box enters again from the opposite side. The less restrictive case of periodic walls is the one adopted here. Periodic models have been used previously by both Clark and Lal[37] and Cosgrove et al.[4] It is appreciated that the polymer end-to-end distance cannot be computed with the periodic model[5] unless one takes into account all lateral shifts; but periodicity is thought unlikely to seriously affect the segment/monomer densities which are of principal interest here. No direct comparative testing of the periodic boundary condition with a full multichain calculation has been attempted nor is knowingly available from other sources (baring a statement by Clark and Lal[37] of agreement between their results and a multichain/periodic cell calculation of H. Okamoto, in a personal communication).

Finally, one considers the possibility of a second surface (of chains) interacting with the first. In the low-ϑ limit, a chain on one surface is unlikely to meet with chains on the second surface so then, to a good approximation, the only extra constraint imposed on a chain configuration is the additional impenetrable surface. For higher values of ϑ there is a greater probability of chains from opposing surfaces encountering one another in the gap. At best this would involve a difficult two-chain simulation. However, if one assumes a great number of contacts, then this interaction can be approximated by replacing chain monomers of the second surface with a hard wall midway between the two. This limits the maximum possible extent of the chains to *half* the bare surface–surface separation, b (see, however, the Discussion).

If any of the above criteria are not satisfied, the configuration should be discarded. However, even for a fairly moderate chain length of, say, 50 it proves to be too time-consuming to obtain an adequate ensemble of completed walks by simple sampling.[41] A biased sampling approach was introduced by Rosenbluth and Rosenbluth[33] (developed and discussed further by McCrackin and others[34-39]) in order to reduce the number of attempts needed for a representative ensemble. The idea proposed is this: tests are conducted at each stage on all 3 possible, subsequent steps in order to eliminate those that fail our criteria; a random selection is *then* made among the remaining possibilities. If, at some point of the walk, *all* three steps do not satisfy the constraints, then the entire walk is discarded. CPU time is lost in the repeated testing, but this loss is compensated for by the fact that fewer new walks need be started.

This selection process produces a biased set of configurations. For instance, if, at the kth step of a walk, a random selection is made among only n_k choices out of the original 3, then these have a *step* probability of $1/n_k$. The ith configuration of N such steps has then a probability of being sampled equal to the product of such likelihoods

$$P_i = \prod_{k=1}^{N} \frac{1}{n_k} \tag{1}$$

This bias of individual configurations is removed by weighting the latter with the reciprocal of this factor.[34] Summed over *all possible* configurations, these probabilities are found to be normalized.

For the case of charged chains on a neutral surface, the most energetically favored configurations are those having the greatest extension out from the surface. These chains will stretch directly out into the solution in order to minimize their presence in an unfavorable, highly charged environment created by charged neighbors. Unfortunately, for very long chains these extended configurations will represent only a small fraction of all possible configurations. In order to sample what might be the important extremes of configurational space, such as these stretched walks, we have included yet another bias. An importance sampling technique[30] gives the extended configurations a greater chance of being included. Eisenriegler et al.,[39] for example, have used a version of this technique for the problem of polymer adsorption where configurations are biased to lie along the surface.

We give steps away from the surface a higher probability of being sampled compared with those parallel to the surface, which, in turn, are given higher probabilities than those toward the surface. That is

$$p_u > p_n > p_d \tag{2}$$

where p_u, p_n, and p_d represent the probabilities of an upward, neutral, and downward step, respectively. These probabilities must naturally satisfy a normality condition here defined by

$$q_u p_u + q_n p_n + q_d p_d = 1 \tag{3}$$

The q's represent the number of choices possible at each step for the three directions (up, down, or neutral). This hierarchy of probabilities, eq 2, is achieved with the introduction of a bias parameter, r, such that

$$\frac{p_n}{p_u} = \frac{p_d}{p_n} = r, \qquad r \le 1 \tag{4}$$

Combining eqs 3 and 4 gives an explicit relation between the p's and q's and r. For the particular case when all *three* steps are possible, we have, as an example

$$p_u = \frac{1}{q_u + q_n r + q_d r^2}, \qquad p_n = r p_u,\ p_d = r p_n \tag{5}$$

When any of the three choices are disallowed, due to either of the above constraints, the explicit form for the hierarchy, eq 5, changes.

This method thus leads to sampling of configurations that have a higher probability of occurrence. For example, if the kth step of a configuration has n_k possible options and the chosen step is given a probability p_k, based on eqs 3 and 4, then once again the probability for that entire configuration is the product of all these step probabilities

$$P_i = \prod_{k=1}^{N} p_k \tag{6}$$

which is higher the smaller the value of r and the more often steps away from the surface appear as options at any stage in a configuration. Clearly, setting r equal to unity reduces eq 6 to eq 1. *All* biasing associated with this set of steps is removed, as in the case of eq 1, by weighting each configuration with the reciprocal of P_i.

As we are primarily concerned with the influence of charge on the chains on the behavior of the system, only electrostatic contributions, evaluated with the mean electrostatic potential, ψ, are included in the energy of the chain in the ith configuration, ϵ_i. Terms related to adsorption energies, van der Waals potentials, internal (trans/gauche) conformational energies, or solvent effects are not considered at this stage. Chain connectivity, interface impenetrability, and excluded volume terms are, of course, implicit in our configuration energy in the sense that only those configurations that satisfy the constraints are included; other configurations are given zero weight (infinite energy). If e is the unit charge and ζ_j is the valence of the jth monomer at a distance z_j^i from the surface, the mean-field electrostatic energy, ϵ_i, of the chain in the ith configuration (from translational invariance, only the z dependence of ψ appears) is given as

$$\epsilon_i = \sum_{j=0}^{N} e\zeta_j \psi(z_j^i) \tag{7}$$

Any thermodynamic property of the chains, g, is then obtained by averaging over the ensemble of configurations weighted by eq 6 and electrostatic energy, eq 7

$$\langle g \rangle = \sum_{i=1}^{M} g_i \frac{\exp(-\beta\epsilon_i)}{P_i} \Big/ \sum_{i=1}^{M} \frac{\exp(-\beta\epsilon_i)}{P_i} \tag{8}$$

where $\beta = 1/kT$.

The canonical partition function for this ensemble of single-chain configurations, Z_p, is given as

$$Z_p = \frac{1}{M_a} \sum_{i=1}^{M} \frac{\exp(-\beta\epsilon_i)}{P_i} \tag{9}$$

The multiplicative factor, $1/M_a$, does not appear in any ensemble average as it cancels between the numerator and denominator. M_a denotes the total number of attempts made, while M denotes the number of accepted configurations. (See the Appendix for a brief discussion of the validity of eq 9.) The corresponding normalized probability for the ith configuration, $\mathcal{P}_i$, is then

$$\mathcal{P}_i = \frac{\exp(-\beta\epsilon_i)}{Z_p} \tag{10}$$

B. Electrostatic Potential. From our simple mean-field point of view, in the absence of any external field, a uni-univalent electrolyte solution is uniformly distributed. However, in charging up of either the walls or the grafted chains, the electrolyte ions will redistribute and the chains uncoil, stretching out from the wall. The classical mean-field treatment of electrolytes at charged interfaces[32] can be generalized to include the effect/presence of charged chains.

We assume the potential, ψ, to be the solution of an "extended" Poisson–Boltzmann (PB) equation

$$\frac{d^2}{dz^2}\psi(z) = -\frac{4\pi}{\epsilon}\left[\sum_i e z_i n_i^0 \exp(-e z_i \beta\psi(z)) + e\zeta n_p(z)\right] \tag{11}$$

Here, the first term is the usual Boltzmann distribution of the mobile ions, $\rho_{ions}(z)$, while the second term represents the distribution of *charge* from the monomers (each having an identical valence of ζ), $\rho_p(z)$. The *monomer* density is defined as an ensemble average of the instantaneous

monomer positions, i.e., from eq 8

$$n_p(z) = \langle \sum_{j=0}^{N} \delta(z - z_j) \rangle \tag{12}$$

The solution of eq 11 must satisfy appropriate boundary conditions. For an isolated surface these are

$$\psi'(0) = -E \text{ and } \psi \to 0 \text{ as } z \to \infty \tag{13a}$$

The first is Gauss' condition for the discontinuity in the field across an interface carrying a surface density of charge, σ, $E = 4\pi\sigma/\epsilon$. The second comes from the electroneutrality condition. For the case of two interacting surfaces at a separation of $2b$, the boundary conditions become

$$\psi'(0) = -E \text{ and } \psi'(b) = 0 \tag{13b}$$

The latter comes from the symmetry of the system (implicitly also from electroneutrality).

Equation 11 cannot be solved analytically for a general monomer density. However, solutions satisfying the boundary conditions, eq 13, exist in integral form and these may be numerically evaluated. They are

$$\psi(z) = \frac{4\pi}{\epsilon} \int_z^\infty ds\ (z - s)\rho_{tot}(s) \tag{14a}$$

and

$$\psi(z) - \psi(0) = \frac{4\pi}{\epsilon} \int_0^z ds\ (s - z)\rho_{tot}(s) - Ez \tag{14b}$$

In eq 14, ρ_{tot} is the total charge distribution, the contents within the square brackets in eq 11.

Both the mobile ion distributions and the chain conformations depend on the potential, ψ. These, as in DLVO theory,[32] must be self-consistent at equilibrium. The way we arrive at an equilibrium here is as follows. Initially, an ensemble of configurations is generated and the distribution of *neutral* monomers calculated. This is then assumed to be a distribution of *charged* monomers and used to determine the electrostatic potential and mobile ion distribution. The potential is then used in generating a new monomer profile which is then held fixed as the potential profile and corresponding ion distributions are updated. This iteration is continued until the relative difference between successive values of a system property is less than a specified tolerance. In particular, we apply the constraint that the relative difference between two consecutive iteration values of the monomer and ion densities at every (discrete) z value be less than 1 part in 1000. What we finally obtain (to a good approximation) is the optimal ionic distribution and equilibrium monomer distribution: these are the minimum free energy states. Covergence of this scheme generally required about 10–20 iterations of the monomer distribution, within which the number of iteractions needed for a converged ionic distribution (or the electrostatic potential) decreased from an initial 40 iterations, with the neutral monomer profile, to zero at self-consistency.

C. Interaction Free Energy. The potential energy of interaction between two surfaces is defined as the difference in the total Helmholtz free energy of the system at a finite separation, $A_{tot}(2b)$, and at infinite separation, $A_{tot}(\infty)$, which we denote by $V_{int}(b)$. This is the interaction free energy, that is, the amount of work needed to bring the plates from infinity to a distance of $2b$.

In turn, the functional form of A_{tot} can be given as the difference in free energy of the system in the final, charged state and in an appropriate reference state, the latter being a bare neutral surface in a uniform electrolyte. This mean-field free energy difference can be formally partitioned in the following manner:

$$A_{tot} = E_{el} - TS_{mix} - TS_p + \Delta U \tag{15}$$

By neglecting all other forms of interaction, for instance solvent effects, we need only consider the electrostatic contribution to the total energy, E_{el}. This term includes information on all electrostatic interactions and has the explicit form[40]

$$E_{el} = \frac{1}{2} \int_v d\mathbf{r}\ [\rho_{tot}(\mathbf{r}) + \sigma(\mathbf{r})]\psi(\mathbf{r}) \tag{16}$$

Notice that in eq 16 we already include the chain energy contribution.

The term TS_{mix} represents the entropy change due to a redistribution of the electrolyte. In the final state the ions are nonuniformly distributed, leading to a decrease in entropy relative to that of the reference uniform ideal gas system, TS^{id}

$$TS_{mix} = T(S - S^{id}) \tag{17}$$

where

$$TS = -kT \sum_i \int_v n_i(\mathbf{r})(\ln(\Lambda_i^3 n_i(\mathbf{r})) - 1)\ d\mathbf{r} \tag{18}$$

and Λ_i is the thermal wavelength of the ith mobile ion species. All terms appearing in eqs 17 and 18 are implicit functions of b.

Accompanying the buildup of charge on the surfaces and chains, there is a transfer of ions from between the bulk and the double layer. With this transfer is a change in the standard free energy of the bulk

$$\Delta U = -\sum_i \mu_i^\circ \int_i (n_i(\mathbf{r}) - n_i^\circ)\ d\mathbf{r} \tag{19}$$

where

$$\mu_i^\circ = kT \ln(\Lambda_i^3 n_i^\circ) \tag{20}$$

is the intrinsic chemical potential (free energy per particle) of the ith species.

Finally, there is the configurational entropy of the polyion chains, TS_p

$$TS_p = 2k_B T\vartheta \ln Z_p + \langle U_p \rangle \tag{21}$$

$\langle U_p \rangle$ is defined as the mean-field approximation to the internal electrostatic energy of the chains

$$\langle U_p \rangle = \int_v \psi(\mathbf{r})\rho_p(\mathbf{r})\ d\mathbf{r} \tag{22}$$

Combining all the contributions in eq 15, we have

$$A_{tot}(b) = \sigma\psi(0) - \int_0^b dz\ \{\psi(z)[\rho_p(z) + \rho_{ions}(z)] + 2k_B T \sum_i (n_i(z) - n_i^\circ)\} - 2k_B T\vartheta \ln Z_p \tag{23}$$

Voight et al.,[42] who also attempted a calculation such as this, considered only E_{el} in their interaction energy, neglecting both the changes in entropy of mixing of mobile ions and any chain configurational entropy.

Results

Before reporting on our principal results on the interaction of surfaces with grafted polyelectrolytes, it is instructive to comment briefly on the accuracy and efficiency of our program.

An earlier report of ours on the influence of surface-attached polyelectrolytes on cell electrophoresis[6] made use of an exact enumeration algorithm to evaluate the complete

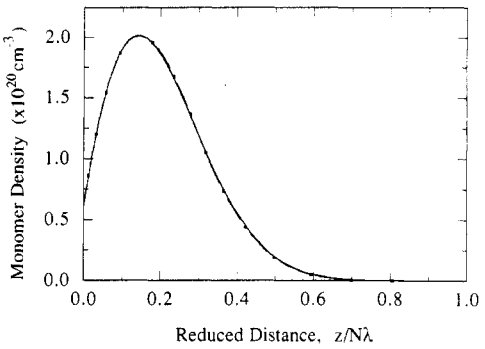

Figure 1. Comparison of a Monte Carlo simulation of 30 000 configurations (- - -) with the exact enumeration result (solid line) of $N = 18$ link chains. The coverage was at 3.75×10^{-4} grafting points per Å^2 with $4\lambda = 25$ Å. The plotted distance is scaled with $N\lambda = 1.125 \times 10^2$ Å, the fully extended chain length. For this test case the chains were assumed uncharged and configurations generated as if they were in steric isolation.

ensemble of configurations for a grafted, all-avoiding chain in similar circumstances. We therefore have at our disposal a convenient check on the accuracy of the Monte Carlo procedure. The two calculation schemes should produce, for instance, approximately the same average monomer profile. In Figure 1 are shown monomer distributions for an 18-bead chain calculated with the exact enumeration scheme resulting in exactly 64 570 082 *accepted* configurations and calculated with our AAW algorithm using 30 000 configurations. These early calculations were carried out on a MicroVax and took 52.3 CPU hours and 41 CPU minutes, respectively. However, all subsequent AAW runs, shown below, were performed on an IBM 3090VF supercomputer using an optimized version of the program (where a similar ensemble of AAWs of an 18-bead chain required only 21 CPU seconds). The conditions assumed for the calculation of our results are given in the figure captions.

As is seen from Figure 1, even with the small number of configurations used, the two density profiles are in remarkable agreement. Not only is our AAW routine correct but it adequately samples *uniform* configuration space. On the other hand, if certain regions of phase space are favored, say by including internal conformation energies, the agreement with the exact enumeration deteriorates. In this case, the simple-sampling random walk method infrequently enters the important region of configuration space where chains have a large number of trans conformations.

In regard to the latter we show in Figure 2 the effect of an importance sampling on the density distribution of monomers in the cases of both neutral and charged chains. Relative to the unbiased calculation, a small value of 0.1 for the bias parameter, r, produces a totally unphysical neutral monomer profile (the dashed, fluctuating curve of Figure 2a). With this fixed value of r (being an extremely strong bias) significantly more configurations are needed to ensure that the biasing is sufficiently compensated and in order to obtain a more stable distribution. What we have chosen to do instead (unless stated otherwise) is to use several bias factors. For example, we implement four different values of r between 0.25 (a fairly strong bias) and 1.0 (no bias) in blocks of configurations of increasing size corresponding to these values, the total again being approximately 100 000. This scheme we suggest is quite reasonable considering that the extended walks represent a relatively small but significant fraction of the complete ensemble. In the absence of a distinguishing potential field, the results show (Figure 2) that the biased monomer profile appears little different from the unbiased case, *except* that

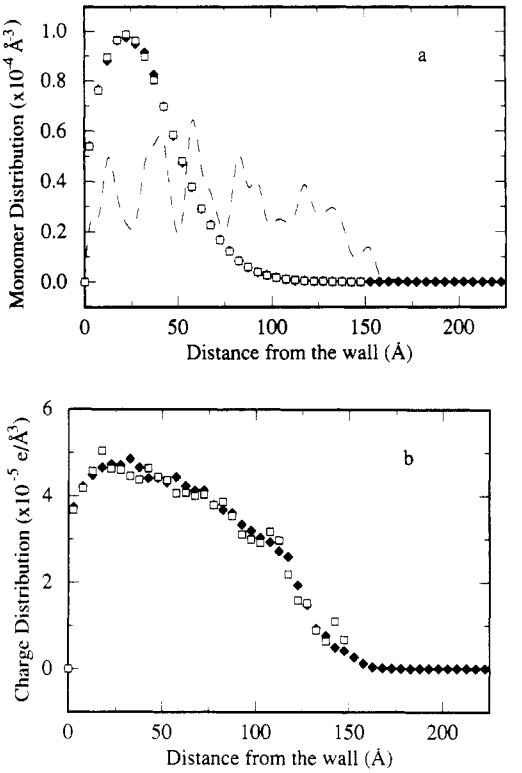

Figure 2. Segment density profiles of an $N = 50$ bond chain of neutral monomers (a) and monomers having a fraction of (negative) charge, $\zeta = -0.5$ (b). The coverage is a dilute 10^{-4} points/Å^2 with $4\lambda = 20$ Å. The open squares correspond to a distribution generated without any bias ($r = 1$), while the distribution represented by filled diamonds was found with a mixed bias. The thin-dashed and highly fluctuating profile shown in (a) is found with a fixed value of the bias parameter, $r = 0.1$. In all cases the number of configurations used was approximately 100 000, and a low-coverge condition was assumed (i.e., a fairly large periodic box). For the charged case an added electrolyte of a concentration of 0.01 M was included.

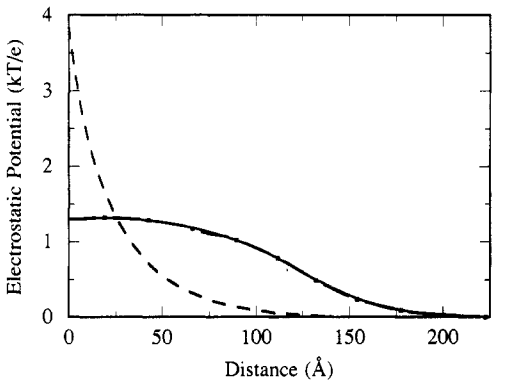

Figure 3. Self-consistent electrostatic profiles (magnitude only) corresponding to the charged monomer distributions shown in Figure 2. The solid lines and dot–dashed lines refer to the biased and unbiased monomer distributions, respectively. The dashed line corresponds to the potential one would find if all the polymeric charge were amassed as a surface charge, $\sigma = e\zeta\vartheta N = 0.0025$ e/Å^2. The electrolyte concentration is 0.01 M.

the unbiased profile ends abruptly at a distance well below the fully extended chain length. The biased distribution on the other hand includes many more of those extended configurations expected to play a bigger role in the case of charged chains. The final profile now includes the distinctive tail in the distribution expected to be important in the case of a charged "brush".

In Figure 3 we show the self-consistent electrostatic profiles corresponding to these charge distributions, both

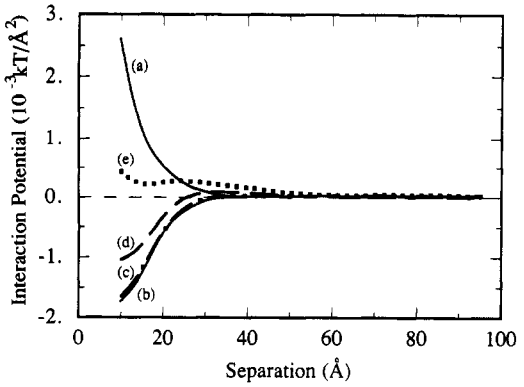

Figure 4. Plots of interaction potential vs surface separation for the case of negative surface charge, $\sigma = -0.08$ C/m^2, and positively charged polyelectrolyte: $N = 10$, $\zeta = +1$, $\vartheta = 0.0005$ graft points/Å^2. The solid curve labeled (a) represents V_{int} for the purely neutral case of uncharged chains grafted to uncharged walls. Curve b is the strict electroneutral case with no added salt; curves c–e are as for curve b except with added monovalent salt at 0.01, 0.1, and 0.5 M concentrations, respectively. Chain configurations were generated with no bias ($r = 1$) and assumed low coverage (no periodic boundaries and no hard wall midway between the surfaces). The number of configurations generated was approximately 50 000.

biased and unbiased calculations, together with the mean electrostatic potential as would be found by replacing all the polyelectrolyte charge with an equivalent amount of surface charge ($\sigma = e \times N \times \zeta \times$ coverage). Potentials for the cases of biased and unbiased distributions appear no different on the scale of this figure, indicating that the electrostatic mean-field is effectively independent of the precise details of the distribution of the monomers. In contrast, the potential profile in the ordinary double-layer case is markedly different as one would expect. Note the slope of the potentials at the wall which earmark the type of distribution assumed. There is a factor of 3 difference between the profiles at the wall, while the chains provide an extended range to the potential.

Recent continuum Monte Carlo simulation and mean-field analysis of a system similar to ours have revealed some remarkable features. Åkesson et al.[28] studied an electroneutral system of two interacting charged surfaces with an intervening short-chain ($N = 10$) polyelectrolyte of opposite charge. They found that the osmotic pressure in the system, evaluated as a function of surface separation, contained a large attractive contribution that dominated over a wide range of separations and parameter values. With our program we can perform a similar calculation and evaluate the interaction free energy for the slightly modified case of *grafted* polyelectrolytes of charge opposite to their grafting surface. For our purposes we only consider one of the surface charge values studied in ref 28, $\sigma = 0.08$ C/m^2 or $\sim$0.005 electron charges/Å^2, which corresponds to a fairly low polymer coverage of approximately 0.0005 chains/Å^2, that is, one chain in every 2000 Å^2. At such a low coverage one may assume that chains on one surface may reach across to the other surface with little or no hindrance from chains on the opposing wall.

In Figure 4 are our results, with and without added salt at three concentrations. Furthermore, we include the case of neutral chains grafted to a neutral wall. The latter results in a purely repulsive interaction and is caused by the compression of the uncharged chain coats. With the approach of the second surface, diminishing regions of available configuration space result in a loss of entropy which, in the absence of any energetic considerations, leads to a straightforward repulsion.

In contrast, we have the interaction profile for the electroneutral case of charged surfaces and oppositely charged grafted chains (Figure 4b). To explain this curve one should firstly consider the surfaces in isolation. Here the chain monomers are on average highly concentrated close to the walls as a result of a strong electrostatic affinity. This represents an entropically unfavorable situation as all the statistical weight is placed on a very small number of energetically favorable configurations. When the two surfaces are at a finite separation, the monomers of chains grafted to one wall have the possibility of residing in the potential *well* near the *other* charged surface; the smaller the separation, the greater this possibility. Thus, some of the more expanded configurations, while having little or no influence in the case of a single surface, also become energetically favorable. As a consequence, in the presence of the second wall, some entropy is salvaged, resulting in a lower free energy per surface compared to a surface in isolation—hence the attraction. At very small separations (a few angstroms) one expects that the strict confinement of the chains produces a repulsion between the surface, as has been found by Åkesson et al.[28]

As salt is added, Figures 4c–e, a progressive screening of both surface charges and monomer charges occurs. One finds that for the surfaces in isolation, the increased screening allows for larger regions of configuration space to become readily accessible to the chains. Basically, the screening of the charges allows the chains to expand out from the wall. Furthermore, at both infinite and finite separations the potential well near either surface is reduced compared to that in the absence of salt. Together these, the diminished well and the already relaxed state of the chains, imply that the entropic gain relative to surfaces in isolation is no longer as large as it was in the no-salt case and decreases further with greater screening. As can be seen from the trend in curves b–e in Figure 4, there is in fact a transition, occurring at a sufficiently high salt concentration, when the presence of the second surface actually leads to a less favorable situation, once again approaching the conditions applying in the neutral case (Figure 4a).

When the surfaces are neutral and the grafted chains charged, a bulk electrolyte solution is required (in the absence of monomer counterions) for electroneutrality to be satisfied. For the case of a polyelectrolyte constrained to be attached to the wall at one end, the most energetically favored configurations are those stretched perpendicular to the wall, extending the charge distribution into the solution (the low-coverage case is shown in Figure 2). At sufficiently large separations of two such surfaces, one then sees a conventional double-layer repulsion extending well beyond that found for the case of a pure surface charge equal to the polyelectrolyte charge (cf. Figures 3 and 5, curves a and d).[44]

The extended configurations, however, represent a relatively small fraction of all possible configurations, so again this situation is not entropically favorable. At intermediate separations the presence of a second potential *barrier* near the opposing wall causes the chains, on average, to "shrink up" on themselves, being repelled by the opposing polyelectrolyte coat. In this case too some entropy is salvaged, this time by the chains, favoring more coiled configurations. This entropy gain results in the appearance of a distinct "shoulder" in the V_{int} curve (Figure 5a) which is totally absent in the ordinary double-layer case (Figure 5c) and which becomes more pronounced as the salt concentration is increased (Figure 5b). At small separations the interaction of surfaces covered with charged

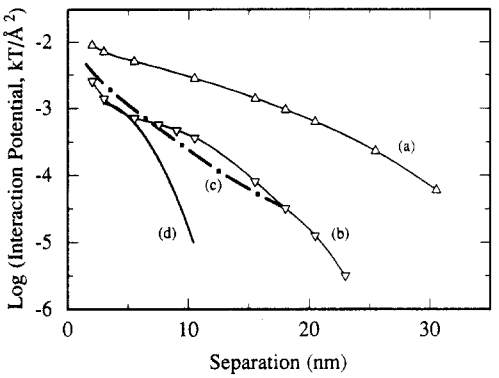

Figure 5. Plots of interaction potential vs surface separation for the case of no surface charge and charged chains: $N = 50$, $\zeta = -0.5$, $\vartheta = 0.0001$ graft point/Å², $4\lambda = 20$ Å. The curve labeled a represents V_{int} found with 0.01 M salt, while curve b for 0.1 M salt present. These are compared with the double-layer interaction free energy found for equivalently charged surfaces, $\sigma = -0.0025$ e/Å², curve c, at 0.01 M salt concentration. Curve d represents V_{int} for neutral brushes. Chain configurations were generated with a mixed bias and at an assumed low coverage (that is, a large periodic box and no hard wall). The number of configurations was approximately 100 000 for all cases. Note that these curves are shown on a log–linear scale.

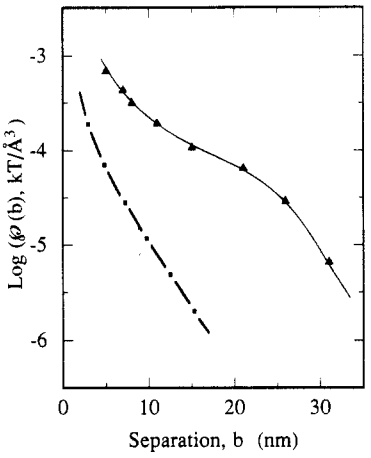

Figure 6. Plots of the approximate pressure function of eq 24, p, vs surface separation for the case of no surface charge and charged chains: $N = 50$, $\zeta = -0.25$, $\vartheta = 0.01$ graft points/Å², $4\lambda = 20$ Å. That is, this figure is for the same case as Figure 5 except at a higher coverage. The salt concentration is 0.01 M. Here we compare the interaction for grafted chains (filled triangles) with that found for equivalently charged surfaces, $\sigma = -0.0125$ e/Å². Chain configurations were again generated with a mixed bias but now at an assumed high coverage (that is, a tight periodic box with a hard wall at the midplane). The number of configurations used was approximately 100 000.

chains remains significantly more repulsive, compared with the ordinary double layer (Figure 5c), as a result of the high cost of compressing the charged coats.

Finally, Figure 6 depicts the interaction of polyelectrolyte coats under the same charge arrangement as in Figure 5 but with the chains at a higher density of coverage. This is also compared to the equivalent double-layer case.

At this higher coverage our difficulty in getting accurate interaction data (see note 44 at end of paper) at large separations is increased. First, V_{int} becomes rather small while the magnitude of the MC statistical errors remains basically unchanged. Although some error is inherent at all separations, the relative error diminishes with decreasing separation. Second, at large separations it becomes progressively harder to obtain self-consistent convergence. In Figure 6 we have taken a step to circumvent the numerical difficulties by not measuring the interaction free energy, but rather an approximate "pressure" function

$$p(b) = \frac{A_{tot}(b - \Delta b) - A_{tot}(b + \Delta b)}{2\Delta b} \tag{24}$$

Thus, we overcome the need to calculate the free energy of an isolated surface.

The trends appearing in Figure 5 are evident too at this high polyelectrolyte coverage for which the interpenetration of chains is not taken into account with the current scheme. The extended range of the double-layer force, the accommodation of the chains at intermediate separations, and the enhanced repulsion at small separations are all reproduced here.

Discussion

Our program gave monomer density values near a surface slightly lower than was given by the exact enumeration,[6] indicating some difficulty in picking up those configurations lying close to the surface. While it is expected to get worse for longer chains, this difficulty is not considered to be a serious handicap to our general conclusions. We should also mention that, as our lattice calculations do not include an accurate monomer size, a "correct" excluded volume treatment, as per the argument of Croxton,[5] is lacking. With this in mind, at no time did we find a discontinuity in our profiles by either method.

Qualitatively, the form of the neutral monomer density profiles agrees with those found by others[3,4,17] in the absence of any direct surface interactions (either attractive or repulsive). There is, however, a significant difference between the shape of these profiles from those found by Cosgrove[4] and Hirz,[7] using the method of Scheutjens and Fleer[43] modified for the grafted chain case, and by Milner et al.,[16] using the mean-field path integral formulation. The latter collection of results pertain to chain lengths on the scale of many hundreds of monomers and usually higher coverages while our calculations have been limited to at most chain lengths of 50 units. This in itself is reason enough to account for the difference in profile shape. With longer chains at high coverages the peak demonstrated here (and also found by Cosgrove et al.[4] under similar conditions) broadens and the density profile "fills out" to become a slowly (indeed quadratically[16]) decaying function of distance from the wall. Under the conditions to which we are restricted it proved impossible to quantitatively compare our results with the "easier" calculation based on the method of Milner et al.[16] For example, no consistent set of (their) parameters would suitably follow a sequence of neutral monomer profiles at different coverages.

Our results on the interaction of polyelectrolyte coats are of most interest. As our program is able to study a variety of different situations of charge, polyion length, and surface coverage, we can study the importance of the different competing effects involved in the interaction process.

Overall, entropic effects produce all the interesting features appearing in our figures. While the approach of a second surface results in a purely monotonic repulsion for the case of neutral chains arising from a loss of available configuration space, in the case of charged chains (with or without surface charges, or either sign) entropic contributions actually lead to attractive terms in the total interaction which may or may not result in overall net attractions, depending on the specific charge conditions.

While it is true that our calculations are outside the regime of validity of Milner et al.'s path integral model,[16] it is nevertheless encouraging that our interaction profiles, shown in Figures 5 and 6, are very reminiscent of those

results found by Miklavic and Marčelja[27] using a simple generalization of this path integral treatment. Clearly, all the essential features have been included.

One item to be pointed out, though, is that at very small separations our results (Figures 5 and 6) indicate no apparent region where the electrostatic interaction of the equivalent surface charge system is similar to the interaction of charged coats, as was found by Miklavic and Marčelja.[27] In their description (as well as in the original) the excluded volume effect is treated in a mean-field way assuming only *average* binary interactions between monomers. While this may be a fair approximation for isolated brushes in the regime of semidilute coverage, at small separations, higher order terms become important, leading to a greater repulsion than is predicted with the current state of that model. At these small separations the increased steric interference will prevent the charged brushes from being compressed effectively to a surface charge, and no similarity in the interaction curves will appear. The present excluded volume treatment via self- and neighbor-avoiding walks on a lattice bears a closer resemblance to reality than this mean-field binary interaction assumption, and Figures 5 and 6 demonstrate the result.

One immediate concern is the implementation of the hard wall constraint midway between the surfaces which we use to mimic the direct steric interaction of the two opposing polyelectrolyte "coats" at high surface coverages. Indeed, this assumption need not correspond to, and may in fact preclude, a true equilibrium state for the system. In such a state, given sufficiently long time for the system to relax, there *would* be significant interpenetration of surface coats of chains. However, the relevant parameter here is really the time of experimental interest compared to the relaxation time for the system. If it is that the relaxation time is much greater than the time of experimental or even practical interest, then the added constraint of a hard wall midway between the coats would not necessarily prevent the system from reaching equilibrium during the duration of an experiment. Some experimental evidence[19-21] suggests that there *is* little or no interdigitation of the chains at these high coverages, supporting the above argument, and adds credibility to our use of the hard wall as a first approximation. Certainly, in respect to the charge distribution on which Figure 6 is based, our approximation is not seriously in error as the polyelectrolyte brushes do on average tend to repel one another. For the situation related to Figure 4, the application of this constraint at a higher coverage may indeed be inappropriate. For instance, it would not have allowed for an attractive interaction at all. Whether this attraction occurs in practice at higher coverages will have to be settled by experiment.

Appendix

For our needs we can consider the simplest case of no importance sampling ($r = 1$) and no electrostatic interaction ($\epsilon_i = 0$); these cases may be treated in a similar manner.

It can be shown that the probability of any allowed configuration Γ, $P(\Gamma)$, is normalized over the ensemble of all possible configurations, N_p. That is

$$\int_{all} d\Gamma\, P(\Gamma) = 1 \tag{A1}$$

The $P(\Gamma)$ will, of course, not be normalized over any smaller sample of M configurations. (The integral expression is used for notational purposes, to distinguish between the complete ensemble of N_p possible configurations and our subset of $M \leq N_p$ configurations.)

An average of an observable, O, over a set of configurations collected according to our scheme (as outlined in the Computational Model section) has the following connection with the full ensemble average:

$$\frac{1}{M_a}\sum_{i=1}^{M} O_i \approx \int_{all} d\Gamma\, P(\Gamma) O(\Gamma) \tag{A2}$$

where M_a is the number of attempts made; those failed configurations ($M_a - M$) give zero contribution to the average. O_i and $O(\Gamma)$ are values for the observable found for the ith sampled configuration and for the Γth configuration in the complete set. That is to say the observable for the ith configuration has implicitly associated with it a bias, P_i, so that the summation actually represents an approximation for a full ensemble average of the *product* of the (unbiased) value $O(\Gamma)$ and the probability $P(\Gamma)$ in the Γth configuration. An immediate consequence of (A2) is that if the observable was taken to be the reciprocal of the probability P_i, that is, the weighting for that configuration, then one obtains an estimate for the total number of possible configurations, $E(N_p)$

$$E(N_p) = \frac{1}{M_a}\sum_{i=1}^{M}\frac{1}{P_i} \approx N_p \tag{A3}$$

However, the number N_p has a statistical thermodynamic interpretation as the partition function for this particular system. Thus, the estimate $E(N_p)$ also provides us with an approximation to the true partition function.

These arguments can easily be generalized to the interacting, importance sampling case giving eq 9 as an estimate to the appropriate partition function.

References and Notes

(1) Napper, D. H. *Polymer Stabilization of Colloidal Suspensions*; Academic Press: New York, 1986.
(2) McDaniel, R. V.; Sharp, K. A.; Brooks, D.; McLaughlin, A.; Winiski, A. P.; Cafiso, D.; McLaughlin, S. *Biophys. J.* **1986**, *49*, 741.
(3) Feigen, R. I.; Napper, D. H. *J. Colloid Interface Sci.* **1977**, *71*, 117.
(4) Cosgrove, T.; Heath, T.; van Lent, B.; Leermakers, F.; Scheutjens, J. M. H. M. *Macromolecules* **1987**, *20*, 1692.
(5) Croxton, C. A. *Fluids Interfacial Phenomena*; John Wiley and Sons: New York, 1986.
(6) Miklavic, S. J.; Ninham, B. W. *J. Theor. Biol.* **1989**, *137*, 71.
(7) Hirz, S. Modeling of Interactions Between Adsorbed Block Copolymers, MSc. Thesis, University of Minnesota, 1986.
(8) Harris, J.; Rice, S. A. *J. Chem. Phys.* **1988**, *88*, 1298.
(9) Björling, M.; Linse, P.; Karlström, G. *J. Phys. Chem.* **1990**, *94*, 471.
(10) de Gennes, P.-G. *Scaling Concepts in Polymer Physics*; Cornell University Press: Ithaca, NY, 1979.
(11) de Gennes, P.-G. *Macromolecules* **1987**, *14*, 1637.
(12) de Gennes, P.-G. *Adv. Colloid Interface Sci.* **1987**, *27*, 189 and references therein.
(13) Edwards, S. F. *Proc. R. Soc. London* **1965**, *85*, 613.
(14) Dolan, A.; Edwards, S. F. *Proc. R. Soc. London*, **1974**, *A337*, 509.
(15) Dolan, A.; Edwards, S. F. *Proc. R. Soc. London* **1975**, *A343*, 427.
(16) Milner, S. I.; Witten, T. A.; Cates, M. E. *Europhys. Lett.* **1988**, *5*, 413; *Macromolecules* **1988**, *21*, 2610; **1989**, *22*, 853.
(17) Muthukumar, M.; Ho, J.-S. *Macromolecules* **1989**, *22*, 965.
(18) The force-measuring technique is described by: Israelachvili, J. N.; Adams, G. E. *J. Chem. Soc., Trans. 1* **1978**, *74*, 975.
(19) Patel, S.; Hadziioannou, G.; Tirrell, M. In *Composite Interfaces*; Ishida, H., Koenig, J. L., Eds.; Elsevier: Amsterdam, 1986.
(20) Patel, S.; Tirrell, M.; Hadziioannou, G. *Colloids Surf.* **1988**, *31*, 157.
(21) Klein, J.; Luckham, P. F. *Nature* **1982**, *300*, 429; **1984**, *308*, 836.
(22) Taunton, H. J.; Toprakcioglu, C.; Fetters, L. J.; Klein, J. *Nature* **1989**, *332*, 712.
(23) Witten, T. Conference Report, 4th International Symposium on Complex Fluids, 1989.
(24) Marra, J.; Hair, M. L. *Macromolecules* **1988**, *21*, 2349, 2356.
(25) Marra, J.; Hair, M. L. *J. Phys. Chem.* **1988**, *92*, 6044.
(26) Marra, J.; Hair, M. L. *J. Colloid Interface Sci.* **1989**, *128*, 511.

(27) Miklavic, S. J.; Marčelja, S. *J. Phys. Chem.* **1988**, *92*, 6718.
(28) Akesson, T.; Woodward, C. E.; Jönsson, Bo *J. Chem. Phys.* **1989**, *91*, 2461.
(29) Christos, G. A.; Carnie, S. L. *J. Chem. Phys.* **1988**, *90*, 439.
(30) Christos, G. A.; Carnie, S. L. *J. Chem. Phys.* **1989**, *91*, 439.
(31) Valleau, J. *Chem. Phys.* **1989**, *129*, 163.
(32) Verwey, E. J. W.; Overbeek, J. Th. G. *Theory of the Stability of Lyophobic Colloids*; Elsevier: Amsterdam, 1948.
(33) Rosenbluth, M. N.; Rosenbluth, A. W. *J. Chem. Phys.* **1955**, *23*, 356.
(34) McCrackin, F. *J. Chem. Phys.* **1967**, *47*, 1980.
(35) Mazur, J.; McCrackin, F. *J. Chem. Phys.* **1968**, *49*, 648.
(36) McCrackin, F. *J. Res. Natl. Bur. Stand., Math. Sci.* **1972**, *76B*, 193.
(37) Clark, A. T.; Lal, M. *J. Chem. Soc., Faraday Trans. 2* **1978**, *74*, 1857.
(38) Kremer, K.; Baumgartner, A. T.; Binder, K. *J. Phys. A: Math. Gen.* **1981**, *15*, 2879.
(39) Eisenriegler, E.; Kremer, K.; Binder, K. *J. Chem. Phys.* **1982**, *77*, 6296.
(40) Jackson, J. D. *Classical Electrodynamics*, 2nd ed.; Wiley: New York, 1975.
(41) Alexandrowicz, J. *J. Chem. Phys.* **1969**, *51*, 561.
(42) Voight, A.; Donath, E.; Heinrich, R. *J. Theor. Biol.* **1982**, *98*, 269.
(43) Scheutjens, J. M. H. M.; Fleer, G. J. *J. Phys. Chem.* **1979**, *83*, 1619.
(44) We note that the computational accuracy diminishes rapidly at large separations so that although the magnitudes calculated and shown in the figures are reliable, it proves to be difficult to obtain the expected asymptotic decay.